Published by Institute of Physics Publishing for SISSA/ISAS
Received: *September 26, 2002*
Accepted: *October 8, 2002*

Diffractive jet production in lepton-hadron collisions

Francesco Hautmann

Physics Department, University of Oregon
Eugene OR 97403, USA, and
Institut für Theoretische Physik, Universität Regensburg
D-93040 Regensburg, Germany
E-mail: hautmann@phys.psu.edu

Abstract: We study jet final states in diffractive deep-inelastic scattering. We present the QCD factorization formula in terms of diffractive parton distributions and discuss its implementation in NLO Monte Carlo generators. We compute NLO predictions for the diffractive jet cross section. We use this calculational framework to discuss theoretical models of the long-distance behavior.

Keywords: QCD, NLO Computations, Deep Inelastic Scattering, Jets.

Contents

1. Introduction

Among the most intriguing results that have come from the HERA lepton-hadron collider are observations of diffraction hard scattering [1]. In these processes, while the short-distance behavior is the one well known from ordinary deep inelastic scattering (DIS), the long-distance matrix elements are much more complex than the usual parton distributions [2, 3] and fully incorporate the dynamics of hadron diffraction.

These diffractive matrix elements, or diffractive parton distributions, have so far been considered mostly in the context of structure functions. One of their key properties, however, concerns the size of the gluon distribution, which, in sharp contrast with the case of ordinary DIS, dominates the quark distributions by one order of magnitude even at low mass scales and large momentum fractions. This enhances the importance of processes, such as the production of jets, that unlike structure functions couple directly to gluons.

The purpose of this paper is to start to analyze systematically the jet structure of diffractive final states in terms of diffractive parton distributions and next-to-leading-order (NLO) short-distance cross sections. A generic jet observable σ will be represented schematically as

$$\sigma[W] = \int f^{(D)} \otimes H \otimes W \, , \tag{1.1}$$

where $f^{(D)}$ is the diffractive parton distribution, H is the hard scattering function, calculable as a power series expansion in α_s, and W is the measurement function, specifying the definition of the observable in terms of the final-state kinematic variables. QCD analyses of diffractive jet production have so far been limited to the leading logarithms [4]–[7]. In this paper, we present the QCD factorization formula that allows nonleading corrections to be systematically included and we carry out the calculation at the NLO. We find that contributions beyond the leading logs are important in the HERA kinematic region.

We argue that, once perturbative corrections are consistently taken into account, jet production can be used to test theoretical models of the long-distance behavior of diffraction scattering. Motivated by a previous comparison [8] of theory with diffractive F_2 data [9, 10], we consider a simple physical picture [3, 8] in which the diffractive gluon distribution results predominantly from color-octet dipoles penetrating the target at small transverse separations of order $1/\kappa$, where $1/\kappa$ represents a color transparency length. This picture gives testable predictions, because the smallness of $1/\kappa$ justifies a perturbative calculation of the β dependence of the distributions. We compute predictions for jet cross sections in this scenario.

The paper is organized as follows. We start in section 2 by presenting the factorization formula for diffractive jet production and its implementation in NLO Monte Carlo generators. This discussion provides a "t-channel" picture of the process, based on the separation of high and low transverse momenta at scale μ, and renormalization-group evolution in μ. In section 3 we examine the diffractive parton distributions. To gain insight into the form of these distributions, it is useful to exploit the intuition that comes from an "s-channel" picture of the process, based on the target rest frame and the light-cone evolution of the parton system created by the operator that defines the distribution. In section 4 we use the results of sections 2 and 3 to compute the diffractive jet cross section, and present numerical results at the NLO. Due to our lack of familiarity with the kinematic cuts employed in the experiments, we leave to the experimental groups the comparison of these results with the data. We summarize and give concluding remarks in section 5.

2. NLO event generators and hard diffraction

In this section we discuss the diffractive factorization formula. Using properties of this formula, we adapt standard NLO Monte Carlo generators for DIS in order to perform NLO calculations of diffractive hard processes.

Consider the diffractive leptoproduction of jets, $e + A \to e' + A' + J + X$, by virtual photon exchange. We parameterize the momenta of the incoming hadron and virtual photon in a collinear reference frame as

$$p_A = \left(p_A^+, \frac{m_A^2}{2p_A^+}, \mathbf{0}\right), \qquad p_\gamma = \left(-xp_A^+, \frac{Q^2}{2xp_A^+}, \mathbf{0}\right), \tag{2.1}$$

where Q^2 is the photon virtuality, x is the Bjorken variable, and we have used lightcone components $p^\pm = (p^0 \pm p^3)/\sqrt{2}$. The Breit frame, in which we will define the jets, is identified by $p_A^+ = Q/(x\sqrt{2})$. We set $y = Q^2/(xS)$, with S the lepton-hadron center-of-mass energy squared. Hadron A' is characterized by the fractional loss of longitudinal momentum $x_{\mathbb{P}} = 1 - p_{A'}^+/p_A^+$ and by the invariant momentum transfer $t = (p_A - p_{A'})^2$.

To be definite, we suppose fixing Q^2 and y in the lepton subprocess, $x_{\mathbb{P}}$ in the diffractive subprocess, and the transverse energy E_T of the jet, whose precise definition is specified below (see section 4). We integrate over t up to a maximum value $t_{\max}$, which we take to be of the order of a GeV. We consider the fourfold-differential jet cross section $d\sigma/[dE_T dQ^2 dy dx_{\mathbb{P}}]$. According to the hard-scattering factorization theorem [2, 3, 11, 12], this cross section is given, up to corrections suppressed by powers of the hard-scattering scale, by

$$\frac{d\sigma}{dE_T dQ^2 dy dx_{\mathbb{P}}}(E_T, Q^2, S, y, x_{\mathbb{P}}) = \sum_{a=g,q,\bar{q}} \int_\beta^1 \frac{d\beta'}{\beta'} \frac{df_a^{(D)}}{dx_{\mathbb{P}}}(\beta', x_{\mathbb{P}}, \mu^2) \times \\ \times \frac{d\hat{\sigma}_a}{dE_T dQ^2 dy}\left(\frac{\beta}{\beta'}, E_T, Q^2, y, \mu^2, \alpha_s(\mu_R^2)\right), \tag{2.2}$$

where β is given by

$$\beta = \frac{Q^2}{x_{\mathbb{P}} y S}, \tag{2.3}$$

$df_a^{(D)}/dx_{\mathbb{P}}$ is the diffractive parton distribution integrated over t and $d\hat{\sigma}_a/\left[dE_T dQ^2 dy\right]$ is the partonic jet cross section, incorporating the hard-scattering function H of eq. (1.1) (through perturbatively calculable matrix elements) and the measurement function W (through the algorithm that defines the jet). The mass scales μ_R and μ are the renormalization and factorization scales.

Eq. (2.2) expresses the separation of short-distance and long-distance contributions to the diffractive jet cross section. It contains two crucial differences compared to the analogous factorization formula for inclusive jet production: a) the distributions $f^{(D)}$, which embody all of the dynamical effects of hadron diffraction, and b) the diffractive kinematics, which enters, through the momentum loss $x_{\mathbb{P}}$, not only in $f^{(D)}$ but also in β, eq. (2.3). The definition of $f^{(D)}$ can be found in [2, 3] and is briefly recalled in section 3.

The important point for practical applications is that the dependence on the hard scale, Q or E_T, factors out of $f^{(D)}$ in eq. (2.2): it is entirely contained in $\hat{\sigma}_a$, as in the inclusive case. Since the left hand side of eq. (2.2) is independent of the factorization scale μ, this also implies that, as in the inclusive case, the evolution of $f^{(D)}$ with μ is given by renormalization-group equations. Because we do not integrate over large t (of the order of the hard scale or higher), the form of these equations is simply DGLAP, without the inhomogeneous term from extra large-t subtractions [2].

We can thus calculate the differential cross section (2.2) to the next-to-leading order using the NLO results that are available for the partonic jet cross sections $\hat{\sigma}_a$, and NLO evolution of the $f^{(D)}$. The cross sections $\hat{\sigma}_a$ start at order α_s. The order-α_s^2 contributions were computed and encoded in Monte Carlo programs by three groups [13, 14, 15]. Two of these programs, DISASTER++ [13] and DISENT [14], have been found [16] to be in good numerical agreement. More recently two other independent programs [17, 18] have appeared. The authors of the program NLOJET++ [18] have also performed a comparison of different codes and found agreement of their results with those of [13, 14]. Any one of these Monte Carlo programs can be used to evaluate the short distance part of eq. (2.2) to NLO.[1]

[1]Note that a numerical discrepancy between DISASTER++ and DISENT has been observed [19] in the case of certain event shape distributions, e.g. the jet broadening, and that DISASTER++ has been identified [20] as the program giving the correct result. As far as we can judge, this discrepancy does not affect the cross sections and the range in transverse energies considered in this paper.

The numerical results that we present in this paper are obtained using DISENT. This program generates DIS events according to a structure reminiscent of parton shower algorithms [21]: first, it generates a parton-model event, with one parton in the final state; then, starting from this and using the dipole subtraction method [14], it generates events with two partons in the final state; then, in a similar way it generates events with three final partons. Contributions to the jet cross section come from events with at least two partons in the final state. For applications to diffractive production, we generate two-parton and three-parton events so that Q^2 and β of the starting event are preserved. Note that if we use variables Q^2, y and β for generating the DIS phase space (any two of which can be fixed), the dependence on the diffractive momentum loss $x_{\mathbb{P}}$ decouples from the convolutions implied by factorization and evolution. We will use this method for the calculations of section 4.

In the next section we turn to the long-distance part of the process.

3. Diffractive parton distributions

The diffractive parton distributions describe the nonperturbative dynamics of the hadronic state, and are defined in [2, 3] in terms of matrix elements of nonlocal quark and gluon field operators. For gluons one has

$$\frac{d\, f_g^{(D)}}{dx_{\mathbb{P}}}(\beta, x_{\mathbb{P}}, \mu^2) = \frac{1}{(4\pi)^3 \beta x_{\mathbb{P}} p_A^+} \sum_X \int_0^{t_{\max}} dt \int dy^- e^{i\beta x_{\mathbb{P}} p_A^+ y^-} \times \\ \times \langle A|\widetilde{G}_a(0)^{+j}|A', X\rangle\langle A', X|\widetilde{G}_a(0, y^-, \mathbf{0})^{+j}|A\rangle \,, \tag{3.1}$$

with

$$\widetilde{G}_a(y)^{+j} = E(y)_{ab} G_b(y)^{+j} \,, \qquad E(y) = \mathcal{P} \exp\left(-ig \int_{y^-}^{\infty} dx^- A_c^+(y^+, x^-, \mathbf{y}) t_c\right), \tag{3.2}$$

where G is the gluon field strength, A is the vector potential, t are the generators of the adjoint representation of SU(3), and E is a color-octet eikonal line operator, with $\mathcal{P}$ denoting the path ordering of the exponential. An analogous definition applies for quarks. Unlike the ordinary (inclusive) parton distributions, the distributions $f^{(D)}$ represent interactions that occur both long before and long after the hard scatter.

The factorization of the previous section implies that the $f^{(D)}$'s can be measured from diffractive DIS data and used in eq. (2.2) to predict jet cross sections. This provides an approach to diffractive jet production that is fully consistent, although agnostic about the form of the matrix elements (3.1), in the spirit of the parton model. Calculations based on this approach are carried out to leading order in [5, 6] and to NLO in this paper. From this point of view, experimental tests of eq. (2.2) to NLO are an important goal of diffractive jet studies.

A complementary approach consists of modeling the dynamics that determines the form of the matrix elements (3.1), and using eq. (2.2) to test these models. It is this point of view that we now wish to take. To this end, we build on the observation [3, 22] that the main qualitative aspects of the data [9, 10] for the diffractive F_2 structure function — steep rise with decreasing $x_{\mathbb{P}}$, flat spectrum in β, positive slope in Q^2 up to $\beta \approx 1/2$ — are all consistent with the hypothesis that the diffractive gluon distribution be dominated by transverse momenta of the order of a (semi)hard scale $M_{\rm SH}$,

$$M_{\rm SH} \sim \mathcal{O}(1\,{\rm GeV})\,. \tag{3.3}$$

This scale has nothing to do with the hard-scattering scale, Q or E_T, which has been factored out and does not appear in $f^{(D)}$. Rather, it represents an intermediate scale between the scale of hard physics and $\Lambda_{\rm QCD}$, whose origin is nonperturbative and associated with the hadron's soft color field.

The physical meaning of the scale $M_{\rm SH}$ was explained in [8] in the reference frame in which the target is at rest. In this frame, the scale $M_{\rm SH}$ is seen to arise as a color-transparency scale, i.e., as the inverse of the maximum size $1/\kappa$ for which the color-octet dipole system created by the operator (3.1) can go through the hadron without breaking it up. The analysis [8] finds that the transparency lengths are smaller for color-octet dipoles than for color-triplet dipoles. The hypothesis of semihard dominance may therefore be better verified for observables (such as jets) that couple directly to the gluon distribution than for structure functions.

Note that the rest frame approach gives an "s-channel view" of the process, characteristic of color-dipole models. Note however an essential difference between the treatment above and standard color-dipole models (see, e.g., ref. [4] for a color-dipole study of diffractive jet production): in the present paper the s-channel picture is applied to the parton system created by the operator in $f^{(D)}$ rather than to the system into which the virtual photon dissociates. That is, it is applied *after* factorizing the hard-scattering subgraph. This difference is relevant, because the factorization provides a framework in which next-to-leading radiative corrections and evolution can be readily implemented. In contrast, such effects are difficult to include in color-dipole models, and evolution is typically taken into account at most to the leading-log level: see, e.g., [23] for a recent study.

The semihard dominance picture leads to testable predictions, because the β dependence of the diffractive parton distributions then becomes calculable by a perturbation expansion. This calculation was first done in [22], using light-cone perturbation theory. We observe that the semihard-scale scenario is common to several different models, including the large-nucleus model [24] and the saturation model [25]. In the following we use the distributions of [8], which incorporate the calculation [22]. At a starting mass scale $\mu = \mu_0$ (with μ_0 of order $M_{\rm SH}$), these distributions have the form

$$\frac{df_g^{(D)}}{dx_{\mathbb{P}}}(\beta, x_{\mathbb{P}}, \mu_0^2) = A_g \frac{1}{x_{\mathbb{P}}^{2\alpha-1}} \varphi_g(\beta)\,, \qquad \frac{df_g^{(D)}}{dx_{\mathbb{P}}}(\beta, x_{\mathbb{P}}, \mu_0^2) = A_q \frac{1}{x_{\mathbb{P}}^{2\alpha-1}} \varphi_g(\beta)\,, \tag{3.4}$$

where the φ's are the perturbatively-computed functions, while A_g, A_q, α have to be determined from the data. The overall normalizations are proportional to the square of the color-transparency scales, $A_g \propto \kappa_g^2 r_A^2$ and $A_q \propto \kappa_q^2 r_A^2$ [8], with r_A the hadron radius.

In eq. (3.4) we have assumed, as is commonly done, a simple factorizing form $x_{\mathbb{P}}^{1-2\alpha}$ for the $x_{\mathbb{P}}$ dependence. This is an ansatz, not a theory result. It is in fact possible that the gluon and the quark distributions have distinct $x_{\mathbb{P}}$ behaviors at low μ [26]. For illustrative purposes in the calculations that follow we limit ourselves to the simple factorizing form.

JHEP10(2002)025

Observe that the larger κ, the larger the parton distribution: large $f_g^{(D)}$ is related to the small size of the color-octet dipoles interacting diffractively [8]. The calculation of the functions φ_g and φ_q shows that the ratio of the gluon and quark distributions is proportional to a large color factor, $C_A^2(N_c^2 - 1)/(C_F^2 N_c) = 27/2$ [22]. In contrast with ordinary DIS, these functions do *not* have a fast fall-off as $\beta \to 1$, resulting in the gluon distribution being large even at large β [22].

As we have seen in section 2, the evolution of the distributions (3.4) with the scale μ^2 is given, up to power-like corrections, by the DGLAP equations, and is to be computed to the NLO, consistently with the accuracy of the partonic cross section. We do this using the moment-space evolution program of [27]. Numerical tables for the resulting distributions in the $\overline{\rm MS}$ scheme are available from `http://zebu.uoregon.edu/~parton/diffpartons`.

The use of the DGLAP evolution equations is consistent with the leading power accuracy of eq. (2.2). However, as emphasized earlier, the diffractive gluon distribution $f_g^{(D)}$ is very large. Then corrections to factorization and evolution of relative order $f_g^{(D)}/(r_A Q)^n$, corresponding to multi-parton correlations, although power-suppressed should likely be significant. Diffractive final states are therefore an especially important case in which to look for signals of behaviors beyond the leading power.

4. Jet cross sections

In this section we calculate the cross section for diffractive leptoproduction of jets by evaluating eq. (2.2) at the NLO. For the short-distance part of the process, we use the Monte Carlo program DISENT as discussed in section 2. For the long-distance part, we use the diffractive parton distributions described in section 3.

We must specify the prescription for converting the final-state partons into jets. Beyond the leading logarithms, this becomes an essential ingredient of eq. (2.2): it is part of the function W in eq. (1.1). Standard, infrared-safe definitions are available both for cone jet algorithms and for $k_\perp$-clustering jet algorithms: see, e.g., [28] for a recent, comprehensive discussion. In the case of inclusive jet measurements [29] in DIS, the H1 collaboration have performed a comparison of different $k_\perp$ algorithms and found the algorithm of [30, 31] to have the smallest hadronization corrections. Since we do not expect any dramatic difference from the diffractive case in this respect, we follow this observation and present results for jets defined using this algorithm. As in [29], we adapt the algorithm, originally defined for hadron-hadron collisions, to the lepton-hadron case, working in the Breit frame. We use the Snowmass recombination prescription [32] to define the transverse energy E_T, pseudorapidity η and azimuth ϕ of the jet in terms of the momenta of its constituent partons. In what follows these kinematic variables are understood to be in the Breit frame.

In the calculations that we present below we integrate the momentum transfer t from $t = 0$ to a maximum value $t_{\rm max} = 1\,{\rm GeV}$. We set the factorization and renormalization scales to $\mu^2 = \mu_R^2 = Q^2$. We set the jet resolution parameter R [30] to the value $R = 1$.

In figure 1 we integrate the cross section (2.2) over y, with $0.1 < y < 0.7$, and plot the triple-differential cross section $d\sigma/[dE_T dQ^2 dx_{\mathbb{P}}]$ versus E_T at a fixed value of $x_{\mathbb{P}}$ for

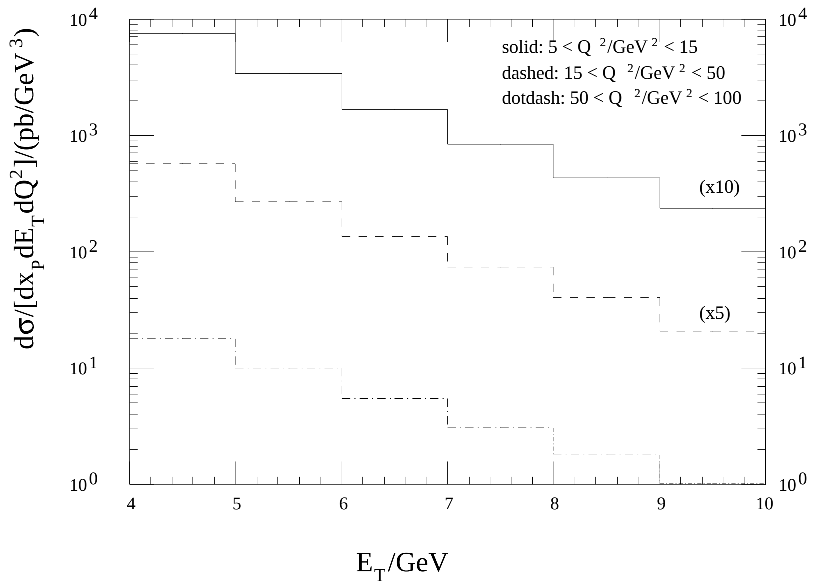

Figure 1: The diffractive one-jet cross section at NLO as a function of the jet transverse energy E_T for different Q^2 bins and $x_{\mathbb{P}} = 0.05$ ($\sqrt{S} = 300\,\mathrm{GeV}$). The energy fraction y is integrated over the interval $0.1 < y < 0.7$. Jets are defined by $k_\perp$-clustering, as specified in the text.

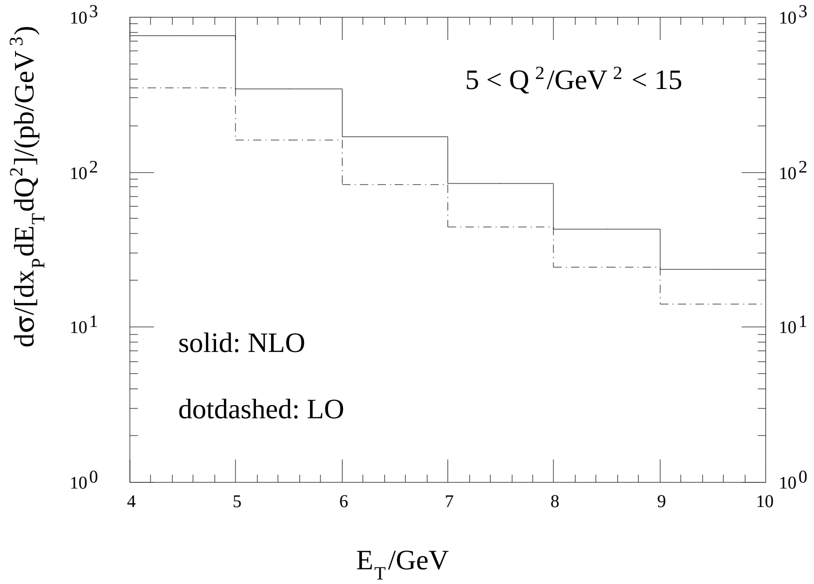

Figure 2: Size of the NLO correction. The values of the kinematic variables and range of integration are as in figure 1 (upper curve).

three different bins in Q^2. The values chosen for the kinematic variables are in the range accessable at HERA.

In order to isolate the quantitative effect of the next-to-leading correction to the hard scattering, in figure 2 we plot the same result as in figure 1 for the lowest Q^2 bin along with the result obtained by including only the leading-order contribution to the hard scattering. The diffractive parton distributions and the value of the running coupling are the same in the two curves of figure 2. The effect is of the order of a factor of 2.

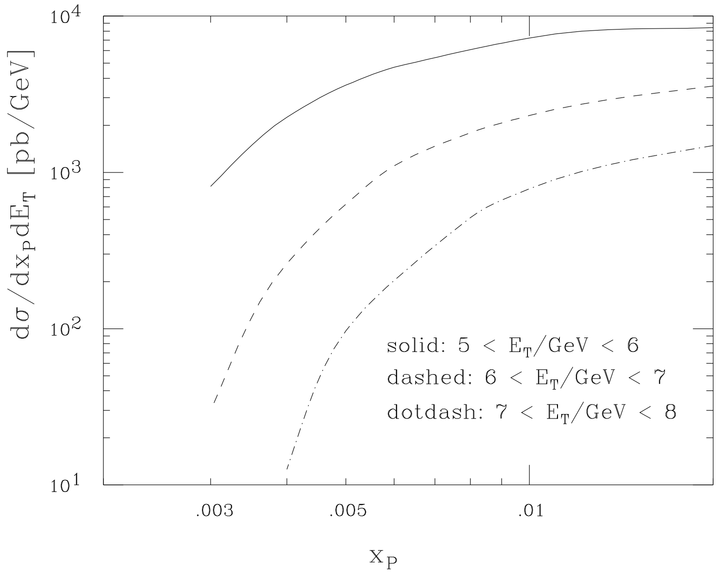

Figure 3: The diffractive one-jet cross section at NLO as a function of the hadron's momentum loss $x_{\mathbb{P}}$ for different jet transverse energies E_T. $\sqrt{S} = 300\,\mathrm{GeV}$; $4\,\mathrm{GeV}^2 < Q^2 < 70\,\mathrm{GeV}^2$; $0.1 < y < 0.7$. Jets are defined by $k_\perp$-clustering, as specified in the text.

Note that from the point of view of the s-channel picture of the process (see, e.g., ref. [4] and discussion in section 3), the LO curve corresponds to the sum of the contributions $\gamma^* \to q\bar{q}$ and $\gamma^* \to q\bar{q}g$, with the latter being by far the dominant one, since $f_g^{(D)} \gg f_q^{(D)}$. The NLO curve corresponds to the first radiative correction to these two contributions. Figure 2 indicates that the radiative corrections (besides evolution) to photon dissociation into $q\bar{q}g$ are important in the HERA region.

The size of the correction raises the question of how to improve the reliability of the perturbation series. Because the short-distance matrix elements are weighted by parton distributions that behave very differently than the ordinary distributions, different physical effects at short distances will dominate the correction compared to the inclusive case. Recall from section 3 that $f_g^{(D)}$ stays large up to large values of β. Then the physical cross section is likely to be sensitive to the behavior of the partonic cross section for small longitudinal momentum fraction and to the tail at finite parton transverse momenta. We leave the analysis of this issue to future investigation.

In figure 3 we show the $x_{\mathbb{P}}$ dependence of the cross section for different E_T bins. We integrate the triple-differential cross section defined above over Q^2, with $4\,\mathrm{GeV}^2 < Q^2 < 70\,\mathrm{GeV}^2$, and plot $d\sigma/[dE_T dx_{\mathbb{P}}]$. Although the distributions $f^{(D)}$ increase with decreasing $x_{\mathbb{P}}$ — see eq. (3.4), with the measured value $\alpha \simeq 1.15$ [9, 10] —, the jet cross section decreases as a result of the reduction in the longitudinal phase space — see eqs. (2.2) and (2.3). This behavior is due to the non-pointlike coupling of jets to the electromagnetic current, and characterizes the measurement of jets with respect to the measurement of the structure function F_2.

Having examined the NLO perturbative corrections, let us now look at the impact of long-distance effects on the jet cross section. To illustrate this, we make use of two fits performed by the H1 collaboration to structure function data [9]. We compare predic-

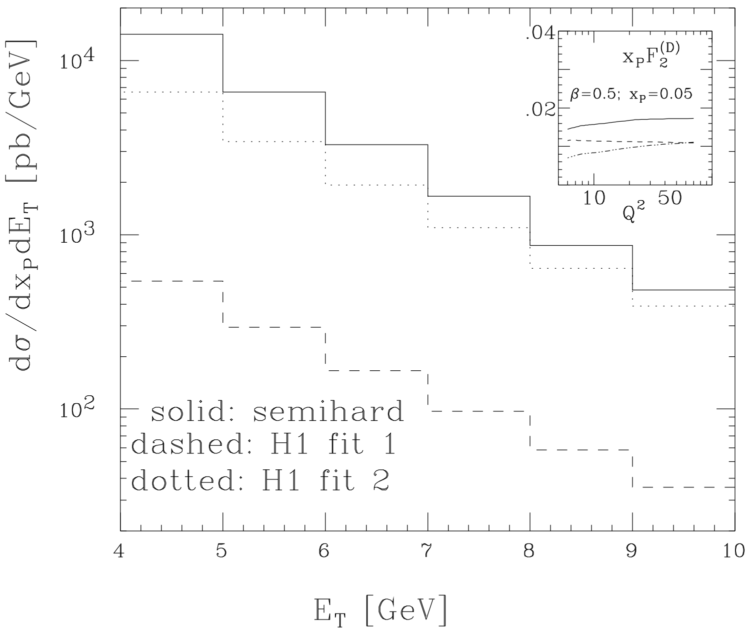

Figure 4: Predictions for the jet cross section corresponding to different diffractive parton distributions. The distributions in the semihard dominance picture (solid curve) are those of [8]; the H1 fit distributions (dashed and dotted curves) are from ref. [9]. The range of integration in Q^2 and y is as in figure 3; $x_{\mathbb{P}} = 0.05$. Inset: results for the diffractive structure function F_2 from the same sets of diffractive parton distributions.

tions based on the diffractive parton distributions in the semihard dominance picture with predictions based on the diffractive parton distributions extracted from the H1 fits. The fit distributions, while compatible with diffractive F_2 data, are representative of different physical pictures of the long-distance process.

Results are given in figure 4. We plot the doubly-differential jet cross section defined above as a function of the jet transverse energy E_T. The solid lines in figure 4 correspond to the same distributions [8] as in the previous figures; the dashed and dotted lines correspond to the fit-1 and fit-2 distributions of H1 [9]. (We recall from [9] that fit-1 distributions are quark-dominated, while fit-2 distributions are gluon-dominated.) The inset in the upper right corner of figure 4 shows the corresponding NLO results for the diffractive structure function F_2, obtained from the same three sets of distributions. The comparison gives a quantitative illustration of how much more sensitive the jet cross section is to long-distance effects than F_2. We may also remark, from the results of figure 2 and figure 4, that while perturbative corrections to diffractive jet rates at HERA are large, on the order of a factor of 2, the effects from different scenarios for the parton distributions (all compatible with F_2 data) are even larger, on the order of a factor of 10. We should likely learn a great deal about the long-distance physics of hard diffraction from the study of jet final states.

5. Summary

In this paper we have presented the factorization formula that relates the diffractive jet-production cross section in DIS to the diffractive parton distributions. Previous studies

JHEP10(2002)025

of diffractive jet leptoproduction have been based on approaches that do not go beyond the leading logarithm approximation. The factorization formula provides a systematic framework that allows arbitrarily nonleading corrections to be included. We have evaluated this formula explicitly to the next-to-leading order.

Using factorization, we have discussed how to adapt standard NLO event generators in order to perform NLO calculations for diffractive jet physics. We have used this method to compute one-jet cross sections. The method is general and can be applied to a variety of final-state observables.

This improved calculational framework can be used to study the diffractive gluon distribution. Building on previous work, and motivated by indications from diffractive F_2 data, we have discussed scenarios for long-distance physics in which the diffractive gluon distribution is dominated by color-transparency lengths of the order of the inverse of a semihard scale, $M_{\rm SH} \sim 1\,\mathrm{GeV}$. In this case the β dependence becomes calculable by perturbation methods, and leads to testable predictions for the jet cross sections.

We recall that the factorization formula is valid up to corrections suppressed by powers of the hard scattering scale. These corrections correspond to multi-parton exchanges and contributions nonlinear in the parton distributions. Since the diffractive gluon distribution is very large, this may overcome the power suppression. We underline the importance of searching for deviations from the leading power particularly in diffractive final states.

We have observed that NLO contributions to the diffractive cross sections are generally large in the HERA kinematic region. In the s-channel language in which color-dipole models are most naturally formulated, this indicates that nonleading-log corrections to photon dissociation into $q\bar{q}g$ states are important. We also noted the possibility that effects from finite parton transverse momenta in the short-distance cross section may be exposed by the large-β behavior of the diffractive gluon distribution. The investigation of these questions is left to future work.

Acknowledgments

I am grateful to D. Soper for collaboration on diffractive physics and for his invaluable advice. I acknowledge discussions with V. Braun, S. Catani, J. Collins, Z. Kunszt and M. Strikman. This work is funded in part by the US Department of Energy.

References

[1] H. Abramowicz, *Diffraction and the pomeron*, *Int. J. Mod. Phys.* **A 15S1** (2000) 495 [hep-ph/0001054].

[2] L. Trentadue and G. Veneziano, *Fracture functions: an improved description of inclusive hard processes in QCD*, *Phys. Lett.* **B 323** (1994) 201:
A. Berera and D.E. Soper, *Behavior of diffractive parton distribution functions*, *Phys. Rev.* **D 53** (1996) 6162 [hep-ph/9509239].

[3] F. Hautmann, Z. Kunszt and D.E. Soper, *Hard scattering factorization and light cone hamiltonian approach to diffractive processes*, *Nucl. Phys.* **B 563** (1999) 153 [hep-ph/9906284].

[4] J. Bartels, H. Jung and M. Wusthoff, *Quark-antiquark-gluon jets in DIS diffractive dissociation*, *Eur. Phys. J.* **C 11** (1999) 111 [hep-ph/9903265].

[5] H1 collaboration, C. Adloff et al., *Diffractive jet production in deep-inelastic $e+p$ collisions at HERA*, *Eur. Phys. J.* **C 20** (2001) 29 [hep-ex/0012051].

[6] ZEUS collaboration, S. Chekanov et al., *Properties of hadronic final states in diffractive deep inelastic $e\,p$ scattering at HERA*, *Phys. Rev.* **D 65** (2002) 052001 [hep-ex/0107052]; ZEUS collaboration, S. Chekanov et al., *Three-jet production in diffractive deep inelastic scattering at HERA*, *Phys. Lett.* **B 516** (2001) 273 [hep-ex/0107004].

[7] A. Edin, G. Ingelman and J. Rathsman, *Unified description of rapidity gaps and energy flows in DIS final states*, *Z. Physik* **C 75** (1997) 57 [hep-ph/9605281].

[8] F. Hautmann and D.E. Soper, *Color transparency in deeply inelastic diffraction*, *Phys. Rev.* **D 63** (2000) 011501 [hep-ph/0008224].

[9] H1 collaboration, C. Adloff et al., *Inclusive measurement of diffractive deep-inelastic $e\,p$ scattering*, *Z. Physik* **C 76** (1997) 613 [hep-ex/9708016].

[10] ZEUS collaboration, J. Breitweg et al., *Measurement of the diffractive cross section in deep inelastic scattering using Zeus 1994 data*, *Eur. Phys. J.* **C 6** (1999) 43 [hep-ex/9807010].

[11] D. Graudenz, *One particle inclusive processes in deeply inelastic lepton-nucleon scattering*, *Nucl. Phys.* **B 432** (1994) 351 [hep-ph/9406274].

[12] J.C. Collins, *Proof of factorization for diffractive hard scattering*, *Phys. Rev.* **D 57** (1998) 3051 [hep-ph/9709499], erratum *ibid.* **D 61** (2000) 019902.

[13] D. Graudenz, *Disaster++ version 1.0*, hep-ph/9710244.

[14] S. Catani and M.H. Seymour, *A general algorithm for calculating jet cross sections in NLO QCD*, *Nucl. Phys.* **B 485** (1997) 291 [hep-ph/9605323].

[15] E. Mirkes and D. Zeppenfeld, *Dijet production at HERA in next-to-leading order*, *Phys. Lett.* **B 380** (1996) 205 [hep-ph/9511448].

[16] C. Duprel, T. Hadig, N. Kauer and M. Wobisch, *Comparison of next-to-leading order calculations for jet cross sections in deep-inelastic scattering*, in proceedings of the Workshop on *Monte Carlo generators for HERA physics*, A.T. Doyle, G. Grindhammer, G. Ingelman and H. Jung eds., Hamburg 1999, p. 142 [hep-ph/9910448].

[17] B. Pötter, *Jetvip 1.1: calculating one- and two-jet cross sections with virtual photons in NLO QCD*, *Comput. Phys. Commun.* **119** (1999) 45 [hep-ph/9806437].

[18] Z. Nagy and Z. Trócsányi,*Multijet cross sections in deep inelastic scattering at next-to-leading order* *Phys. Rev. Lett.* **87** (2001) 082001 hep-ph/0104315.

[19] G.J. McCance, *NLO program comparison for event shapes*, in Proceedings of the Workshop on *Monte Carlo Generators for HERA Physics*, A.T. Doyle, G. Grindhammer, G. Ingelman and H. Jung eds., Hamburg 1999, p.151 [hep-ph/9912481].

[20] M. Dasgupta and G.P. Salam, *Resummation of the jet broadening in DIS*, *Eur. Phys. J.* **C 24** (2002) 213 hep-ph/0110213.

[21] M.H. Seymour, *The DISENT Program*, http://hepwww.rl.ac.uk/theory/seymour/nlo/.

[22] F. Hautmann, Z. Kunszt and D.E. Soper, *Diffractive deeply inelastic scattering of hadronic states with small transverse size*, *Phys. Rev. Lett.* **81** (1998) 3333 hep-ph/9806298.

JHEP10(2002)025

[23] J. Bartels, K. Golec-Biernat and H. Kowalski, *A modification of the saturation model: dglap evolution*, *Phys. Rev.* **D 66** (2002) 014001 [hep-ph/0203258].

[24] W. Buchmüller, T. Gehrmann and A. Hebecker, *Inclusive and diffractive structure functions at small x*, *Nucl. Phys.* **B 537** (1999) 477 [hep-ph/9808454].

[25] K. Golec-Biernat and M. Wüsthoff, *Diffractive parton distributions from the saturation model*, *Eur. Phys. J.* **C 20** (2001) 313 [hep-ph/0102093].

[26] F. Hautmann, *$Q\bar{Q}g$ contribution to diffractive J/ψ electroproduction*, *J. High Energy Phys.* **04** (2002) 036 [hep-ph/0105082].

[27] R.K. Ellis, F. Hautmann and B.R. Webber, *QCD scaling violation at small x*, *Phys. Lett.* **B 348** (1995) 582 [hep-ph/9501307].

[28] G.C. Blazey et al., *Run II jet physics*, in Proceedings of the Workshop on *Physics at Run II: QCD and Weak Boson Physics*, Batavia 1999, p. 47 [hep-ex/0005012].

[29] H1 collaboration, C. Adloff et al., *Measurement and QCD analysis of jet cross sections in deep-inelastic positron proton collisions at $\sqrt{s}$ of 300 GeV*, *Eur. Phys. J.* **C 19** (2001) 289 [hep-ex/0010054].

[30] S.D. Ellis and D.E. Soper, *Successive combination jet algorithm for hadron collisions*, *Phys. Rev.* **D 48** (1993) 3160 [hep-ph/9305266].

[31] S. Catani, Y.L. Dokshitzer, M.H. Seymour and B.R. Webber, *Longitudinally invariant $K(t)$ clustering algorithms for hadron-hadron collisions*, *Nucl. Phys.* **B 406** (1993) 187.

[32] J. Huth et al., in Proceedings of the Workshop *Research directions for the decade: Snowmass 1990*, E.L. Berger ed., World Scientific 1992, p. 134.

JHEP10(2002)025